Nano World Journal

https://doi.org/10.17756/nwj.2023-s3-090

Research Article

Open Access

# Experimental Investigation of Wear Behavior of Aluminum Metal Matrix Composites Synthesized with Gr-$Fe_3O_4$-$B_4C$ Nanoparticles

**Anoop Joshi[1], Vijay Ananth Suyamburajan[1*], Kumar Ramar[2] and Ajith Arul Daniel Selsam Chandradoss[1]**

[1]*Department of Mechanical Engineering, Vels Institute of Science, Technology and Advanced Studies, Chennai, Tamil Nadu, India*

[2]*Department of Mechanical Engineering, Eritrea Institute of Technology, Eritrea*

**[*]Correspondence to:**
Vijay Ananth Suyamburajan
Department of Mechanical Engineering,
Vels Institute of Science, Technology and Advanced Studies,
Chennai, Tamil Nadu, India.
**E-mail:** ssvijayananth@gmail.com

**Received:** July 28, 2023
**Accepted:** October 17, 2023
**Published:** October 19, 2023

**Citation:** Joshi A, Suyamburajan VA, Ramar K, Chandradoss AADS. 2023. Experimental Investigation of Wear Behavior of Aluminum Metal Matrix Composites Synthesized with Gr-$Fe_3O_4$-$B_4C$ Nanoparticles. *NanoWorld J* 9(S3): S490-S495.



Published by United Scientific Group

## Abstract

The current investigation focuses on the wear behaviour of an LM25 aluminum alloy that has been strengthened with boron carbide ($B_4C$) and graphite (Gr) particles using a stir casting manufacturing technique. In order to prepare the LM25 aluminum metal matrix composites (AMMCs), $B_4C$ and Gr reinforcement are added in amounts of 2, 4, and 6 weight percent with different grain sizes ($B_4C$ = 40 µm, Gr = 7 µm). The examination of the wear behavior, wear loss, and coefficient of friction (CoF) characteristics of primed samples was conducted utilizing a pin-on-disk wear test apparatus at room temperature. In order to evaluate the wear behavior of LM25-$B_4C$-Gr composites, loads of 10 N, 20 N, and 30 N, speeds of 6 m/s, and sliding distances of 2000 m were taken into account. The composites' worn surface was inspected using a field emission-scanning electron microscope (FE-SEM). It was observed that the wear rate, CoF, and FE-SEM images of AMMCs were improved by the incorporation of reinforcing $B_4C$ and Gr particles.

## Keywords

LM25, Stir casting, Wear, Coefficient of friction, Field emission-scanning electron microscope

## Introduction

Aluminum and its alloys are one of the most preferred materials and light weight materials because of its lower density in evaluation to aluminum and steel [1-3]. Aluminum alloys are frequently utilized in particular components of aerospace, automobile, and marine applications, and recent days many researchers are annoying to substitute the predictable material like steel and aluminum with aluminum [4, 5]. The limitation of aluminum alloy reveals lower strength and poor ductility and, which can be conquer by the totaling of nano-reinforcements [6, 7]. An addition of nano-reinforcements in aluminum matrix enhances properties like strength, hardness, stiffness, and wears resistance [8].

AMMCs are acquiring attention due to their lightweight capabilities. Furthermore, they exhibit favorable characteristics such as weldability, machinability, thermal stability, castability, specific mechanical properties, and resistance to electromagnetic radiation [9-11]. However, the limitations of AMMCs stem from their low ductility, modulus, and inadequate corrosion resistance. These AMMCs find applications in various areas such as power tools, computers, aerospace technology, automotive industry (including transfer case, radiator support, instrument panel beam, communication, consumer products, and steering components). To enhance the strength for structural purposes, the inclusion of hard and tough ceramics into aluminum alloys is accomplished through appropriate manufacturing techniques [12]. Aluminum LM25D cast alloy is employed in various commercial components such as covers, housings, handheld tools, sporting goods, computer parts, mobile and telephones, household equipment, and automobile components. The main utilization of the LM25 aluminum alloy lies in the production of profitable structural components due to its exceptional combination of room-temperature strength and ductility [13, 14]. However, its usage is constrained to the internal parts in the cast products, as the reticular β-Mg17Al12 phases found at grain boundaries and dendritic arms negatively impact mechanical properties [15]. Grain refinement plays a vital role in enhancing the mechanical properties of aluminum alloys, particularly those with a close-packed hexagonal structure. Grain refinement effectively reduces hot tearing propensity and shrinkage porosity while improving creep properties and corrosion resistance [16].

Different types of reinforcement can be utilized for the mixture of AMMCs like Gr, tungsten carbide (WC), TiC, titanium diboride ($TiB_2$), silicon carbide (SiC), $ZrB_2$, $Al_2O_3$, and $B_4C$ [17, 18]. Among these $B_4C$ is deemed as superior properties like high hardness; refractoriness and wear resistance are used as a reinforcement material of AMMCs. Many researchers used as a single reinforcement, but if additionally add one more reinforcement also AMMCs achieved superior mechanical properties. For current research used as one more reinforcement as Gr. Due to its inexpensive cost and easy availability, hexagonal lattice crystal structure graphite has been utilized. Applications for self-lubricating composites with Gr reinforcement can be found in hostile or vacuum environments where liquid lubrication is challenging or impossible [19].

Singh et al. [20] studied wear behavior analysis of LM25-$B_4C$ composite was fabricated by friction stir processing. Effect of the $B_4C$ particles added in LM25 matrix as enhanced wear resistance and microhardness. Patle et al. [21] conducted the fabrication and analysis of the wear behavior of a composite material consisting of LM25-$B_4C$. The presence of the reinforcement in the matrix materials had a significant impact and resulted in superior wear resistance. Mohammadi et al. [22] focused on the reinforcement of LM25-Mg alloy with $B_4C$, and their findings indicate that the LM25-x$B_4C$ composite can be considered as an exceptional material, particularly in the aerospace and automotive engineering sectors where high compressive strength and wear-resistant components are of great importance. Patle et al. [23] carried out the preparation of LM25/$B_4C$ surface composites under both air and argon gas atmospheres. The outcomes of their study pave the way for the development of lightweight material surface composite systems like LM25/$B_4C$, which can be efficiently and robustly applied in a controlled environment. According to Chinthamani et al. [24], the addition of $B_4C$ as a reinforcement in a Mg matrix leads to an increase in both the wear resistance and strength of the base material. Additionally, the wear resistance of nano $B_4C$ reinforced composites surpasses that of the unreinforced alloy. Regardless of the applied stress, the specific wear rate of the composites and the base metal increases. The increase in applied stress often leads to a shift in delamination wear from abrasion to adhesion. Pitchayyapillai et al. [25] conducted an examination on the effects of reinforcement $B_4C$ on the hardness, compression, and flexural strength of the LM25 aluminum alloy composite. The presence of the enhanced ceramic phase in the composites resulted in the testing results indicating a higher level of hardness compared to the basic alloy. Jeffrey et al. [26] conducted research that involved conducting a tensile test using a universal testing machine, performing a microhardness test using a Vickers hardness tester, and utilizing an optical microscope to investigate the microstructure of LM25/$B_4C$ composites.

The hybrid composite LM25D-SiC-Gr, which was created by Khatkar et al. [27], exhibited the most favorable wear properties. The investigation of worn surfaces using scanning electron microscope (SEM) and energy dispersive X-ray spectroscopy techniques confirmed that delamination was the primary wear mechanism for the LM25D-SiC-Gr hybrid composites. Sahoo et al. [28] developed an *in-situ* LM25+TiC-$TiB_2$ composite, resulting in significant grain refinement and a redistribution of the β-Mg17Al12 phase along the grain boundaries. This process led to simultaneous improvements in strength and ductility, as a result of the combined effects of *in-situ* reinforcing and grain refining achieved through the process. Aydin et al. [29] investigated LM25 aluminum matrix composites enhanced with $TiB_2$ particles, which were fabricated using the hot-pressing technique in powder metallurgy. The microstructure, density, hardness, wear resistance, and mechanical characteristics of the specimens were analyzed. The presence of $TiB_2$ particles enhanced both the ultimate compressive strength and compressive yield strength by 0.2 percent; however, the ultimate compressive strength decreased when the $TiB_2$ content reached 20 weight percent, both oxidative and abrasive wear processes are in existence. Deng et al. [30] utilized stir casting to prepare the LM25 aluminum matrix composites reinforced with submicron-SiC particles. The incorporation of submicron-SiC particles facilitated the enhancement of the elastic modulus, thermal stability, microhardness, and 0.2 percent yield strength.

The level of submicron-SiC particles increased concurrently with the yield strength and ultimate tensile strength, nevertheless, they both declined after surpassing a volume percentage of 2 for the SiC particulate. Submicron size $SiC_p$-LM25 aluminum composite was developed by Deng et al. [30] through the implementation of stir casting, thereby augmenting the thermal stability, microhardness, elastic modulus, and yield strength. According to Zhang et al. [31], the processing of nano-$SiC_p$/LM25 composites results in an augmentation of the workability of LM25 at high temperatures as a result of elevating the processing strain rate's upper limit and enabling low temperature processing through the reduction of the temperature's lower limit. However, the additional particles do induce a side effect by expanding the base alloy's instability region to a lower strain rate and an even higher temperature. Guler et al. [32] conducted an examination on the impact of graphene nano-sheets (GNS) on the mechanical and corrosion characteristics of composites based on AZ61 and LM25. The findings have demonstrated that the compressive strength of the composites in both the AZ61 and LM25 matrix alloys increased as the quantity of GNS increased. The corrosion susceptibility was found to be highest in the AZ61 and LM25 matrix composites that contained 0.5 weight percent of GNS. In order to achieve good corrosion resistance, the Mg matrix must have a specific ratio of GNS content. For the current research, LM25 was selected as the matrix material and was reinforced with nanoparticles such as $B_4C$ and Gr using the stir casting method. Stir casting is considered the most cost-effective, highly innovative, and simplest process for fabricating composites. It is a splendid approach for achieving a uniform distribution of reinforcement. According to Arivukkarasan et al. [33], the addition of WC particles was found to be evenly dispersed throughout the matrix. This was attributed to the effective stirring action and the proper implementation of stir casting method during the casting process.

Based on the literature studies, the matrix material LM25 reinforced with $B_4C$ and Gr particles has not been carried out. Hence, the major objective of the research is to prepare the LM25 aluminum matrix to reinforce with $B_4C$ and Gr hybrid composites developed by one of the simplest liquid metallurgies as stir casting route. After that, hybrid composites involve wear and FE-SEM testing and improve wear resistance.

# Experimentation

## Materials

The LM25 Mg alloy has been selected as the matrix alloy and was purchased from Sebaas Aluminium Alloys (p) Ltd., located in Virudhunagar, Tamil Nadu (India). The chemical composition of the LM25D Mg alloy is provided in table 1. The main reinforcement consists of $B_4C$ particles, while the additional reinforcement consists of Gr particles supplied by Salem Steel Plant (Tamil Nadu, India). The details regarding the materials, including their density and grain size, can be found in table 2. For this particular investigation, the weight percentages of $B_4C$ and Gr varied as 2%, 4%, and 6% for the production of LM25-$B_4C$-Gr hybrid AMMCs using the stir casting method [27, 34].

**Table 1:** The chemical composition of LM25 Mg alloy.

| | |
|---|---|
| Aluminum, Al | 8.3 - 9.7 |
| Manganese, Mn | 0.15 - 0.50 |
| Zinc, Zn | 0.35 - 1 |
| Silicon, Si | 0.1 |
| Copper, Cu | 0.03 |
| Iron, Fe | 0.005 |
| Nickel, Ni | 0.002 |
| Others, each max | 0.02 |
| Magnesium, Mg | Remaining |

**Table 2:** Details of reinforcement materials.

| Materials | $B_4C$ | Gr |
|---|---|---|
| **Purity (%)** | 99.9 | 99.9 |
| **Average grain size (µm)** | 40 | 7 |
| **Density (g/cc)** | 2.52 | 2.1 |

## Stir casting

The stir casting method, which is one of the renowned liquid metallurgy techniques, was employed to fabricate the composite due to its economical nature [35]. The initial phase involves the matrix material being contained in a Gr crucible and liquefied within a stimulating furnace. As for the LM25 Mg alloy, it is liquefied under an inert gas atmosphere to prevent element rejoining and facilitate casting production. In order to achieve the desired molten metal condition, pre-warmth reinforcements are consistently added to the molten metal. To ensure uniform dispersion of the reinforcement particles, the molten metal is then continuously swirled at a rate of 450 rpm for duration of 8 min. Subsequently, the molten metal is poured into pre-warmth steel molds with dimensions of 100 x 30 mm at a temperature of 765 °C, and left to solidify, as depicted in figure 1 [34].

**Figure 1:** Stir cast specimen.

## Wear experiment

A pin-on-disc wear tester, specifically the DUCOM TR-20, which is readily available in the Mechanical Engineering Department of Adhi College of Engineering and Technology in Kanchipuram (Tamil Nadu, India), was utilized for the purpose of conducting the wear experiment. It is worth noting that the wear testing machine is visually depicted in figure 2. It is of utmost importance to mention that the wear tests were carried out in strict accordance with the guidelines set forth by ASTM G99. In order to conduct the wear testing, a pin with a diameter of 6 mm and a length of 25 mm was meticulously extracted from the sintered samples. Notably, all of the samples were endowed with a meticulously polished and impeccably finished surface, which served as the platform for the subsequent wear tests. To accomplish this, the surface of the samples underwent a meticulous rubbing process against emery sheets of varying grades, ranging from grade 320 to grade 1000. Upon the successful completion of the wear tests, a fine alumina powder was employed for the purpose of polishing the fabric. All wear tests were conducted at room temperature and in an open environment. The pin (sample) surface was worn down by rubbing it against the EN91 hardened steel disc. The distance between the pin wear surface and the disc center, rotational speed, and load were all maintained at constant values of 15 N, 220 rpm, and 55 mm, respectively. The wear tests were continuously carried out for a duration of ten minutes. Two tests were performed for each composite to validate the results (Figure 3). Wear examination was conducted on four specimens under the same environmental conditions as indicated in table 3 [34-39], with three different loads of 10, 20, and 30 N, a sliding distance of 2000 m, and a velocity of 6 m/s.

## FE-SEM

FE-SEM possesses an extensive depth of field, rendering it capable of providing elemental information at magnifications spanning from 10xs to 300,000xs. In contrast to conventional SEM, FE-SEM possesses a multitude of applications. These include the examination of semiconductor device cross sections for gate widths, gate oxides, layer thicknesses, and fabrication details, as well as the measurement of small contamination feature geometry and elemental composition. The electron gun within a scanning electron microscope contains a field-emission cathode, which generates narrower probing beams at both low and high electron energies. This results in heightened spatial resolution and decreased sample charging and damage. The testing setup for FE-SEM is depicted in figure 4.

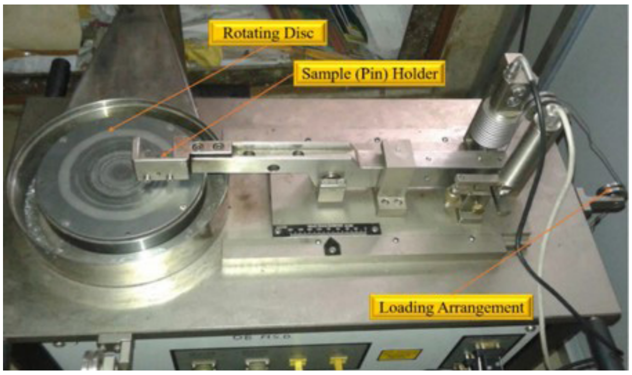

**Figure 2:** Pin-on-disc wear testing machine.


**Figure 3:** The images of the wear test pins.


**Figure 4:** FE-SEM.

**Table 3:** Wear test parameters.

| | |
|---|---|
| Load (N) | 10, 20, 30 |
| Sliding velocity (m/s) | 6 |
| Sliding distance (m) | 2000 |
| Dimension (Diameter x length, mm) | 30 x 100 |

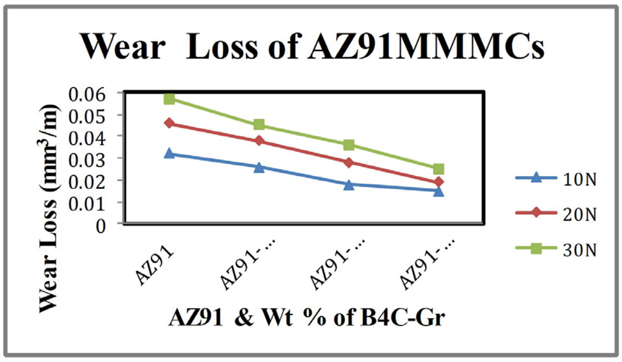

**Figure 5:** Wear loss vs Effect of LM25 alloy and 2, 4, 6% ($B_4C$-Gr) reinforcement.

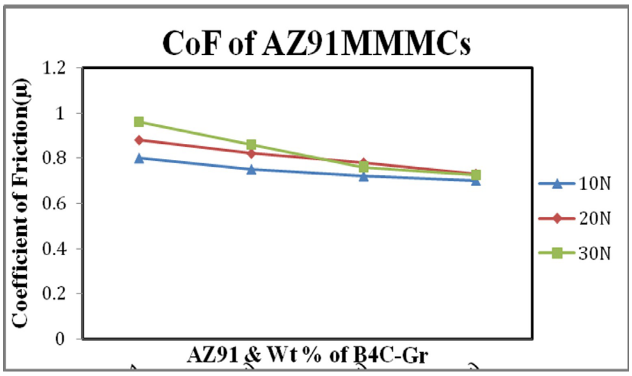

**Figure 6:** CoF vs Effect of LM25 alloy and 2,4,6% ($B_4C$-Gr) reinforcement.

## Results and Discussion

### Wear analysis

Dry sliding wear analyses based on the factors: weight loss, applied force, and sliding distance was used to calculate the specimen's wear loss. Figure 5 depicts the variation in wear loss of LM25-$B_4C$-Gr composites with the addition of 2, 4, 6% $B_4C$ and Gr reinforcements. The sample made of the aluminum alloy LM25 had the most wear loss. Due to the reinforcement particles resistance to scratching, the wear rate reduced when $B_4C$ and Gr were added. This resulted from the elimination of $B_4C$ and Gr particles that were agglomerated and weakly bound. As a result, LM25-$B_4C$-Gr composites reinforced with 6 volume percent $B_4C$ and Gr particles had the lowest wear rate, which was 0.015 $mm^3/m$. CoF is:

$$ì = \frac{PF}{P}$$

Where, μ is CoF, PF is pressure force, and P is applied load.

While the speed and distance were augmented to 2000 m, the $B_4C$-Gr reinforcements and applied load showed a reduction. The of LM25 alloys diminishes as the $B_4C$-Gr virtually rises. It is simple to think that sliding speeds were used to get low CoF values for AMMCs. As shown in figure 6, the maximum value of is 0.96 for LM25 alloy and the minimum value of is 0.725 for LM25-$B_4C$-Gr composites. With the aim of further growing at sliding speed, the current investigation unfolds up for development in the AMMCs specimens as the applied stress increases [40-42].

### FE-SEM

Figure 7 displays FE-SEM graphs of the worn surface following pin-on-disc wear testing. The wear hatching lines of the pure aluminum samples are continuous and have equal spacing, as can be seen in figure 7a. The spacing in the worn hatching lines of the $B_4C$-Gr reinforced samples, however, is discontinuous and non-uniform, as seen in figure 7b to 7d. $B_4C$ and Gr particles that prevent scratching are the cause of the irregular and non-uniform wear hatching lines in LM25 AMMCs. The result shows the organization of artificial warp, fine ruts, rubble, micro-ruptures, and ditch holes as glowing as the route in the direction of more substance removal com-

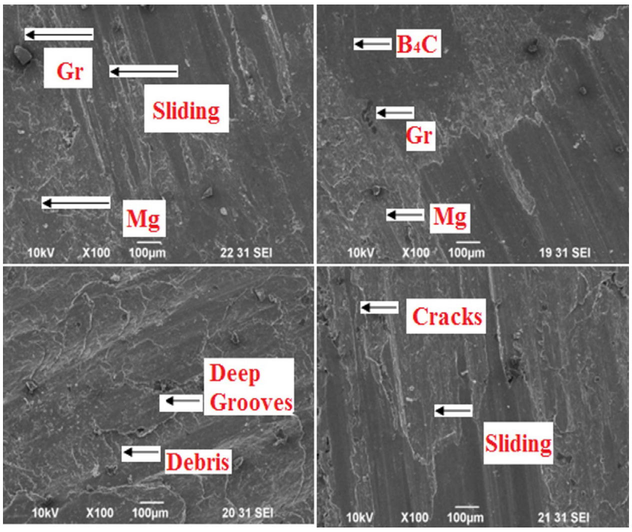


**Figure 7:** FE-SEM micrographs of LM25-$B_4C$-Gr composite.

mencing the surface due to the significant force at the point of contact [43, 44].

## Conclusions

The following conclusion can be drawn from the present investigation.

- The LM25-$B_4C$-Gr composite was created via the stir casting process. Investigations were done into how $B_4C$-Gr reinforcements affected wear behavior.
- The examination of wear loss showed that adding $B_4C$-Gr reinforcements greatly enhanced the wear loss of the AMMCs, which was reduced by 6%. The wear rate for $B_4C$ and Gr particles was the lowest, at 0.015 $mm^3/m$.
- The worn hatching lines in the $B_4C$-Gr reinforced samples FE-SEM graphs, however, had discontinuous and irregular spacing.
- The outcome demonstrates how synthetic warp, fine ruts, rubble, micro-ruptures, and ditch holes were set, as glowing as the lane taken by additional amounts of material to be removed from the samples as a consequence of the strength that was applied initial point of make contact with the facade.

## Acknowledgements

None.

## Conflict of Interest

None.

### References

1. Cai H, Guo F, Su J, Liu L, Chen B. 2018. Study on microstructure and strengthening mechanism of AZ91-Y magnesium alloy. *Mater Res Express* 5(3): 036501. https://doi.org/10.1088/2053-1591/aab0b7
2. Babu BS, Prathap P, Balaji T, Gowtham D, Adi SS, et al. 2020. Studies on mechanical properties of aluminum based hybrid metal matrix composites. *Mater Today Proc* 33: 1144-1148. https://doi.org/10.1016/j.matpr.2020.07.342
3. Ghasali E, Alizadeh M, Niazmand M, Ebadzadeh T. 2017. Fabrication of magnesium-boron carbide metal matrix composite by powder metallurgy route: comparison between microwave and spark plasma sintering. *J Alloys Compd* 697: 200-207. https://doi.org/10.1016/j.jallcom.2016.12.146
4. Penther D, Ghasemi A, Riedel R, Fleck C, Kamrani S. 2018. Effect of SiC nanoparticles on manufacturing process, microstructure and hardness of Mg-SiC nanocomposites produced by mechanical milling and hot extrusion. *Mater Sci Eng A* 738: 264-272. https://doi.org/10.1016/j.msea.2018.09.106
5. Turan ME, Zengin H, Cevik E, Sun Y, Turen Y, et al. 2016. Wear behaviors of $B_4C$ and SiC particle reinforced AZ91 magnesium matrix metal composites. *Int J Mater Metall Eng* 10(9): 1224-1227.
6. Kumar A, Kumar S, Mukhopadhyay NK. 2018. Introduction to magnesium alloy processing technology and development of low-cost stir casting process for magnesium alloy and its composites. *J Magnes Alloys* 6(3): 245-254. https://doi.org/10.1016/j.jma.2018.05.006
7. Zhang X, Zhang Q, Hu H. 2014. Tensile behaviour and microstructure of magnesium AM60-based hybrid composite containing $Al_2O_3$ fibres and particles. *Mater Sci Eng A* 607: 269-276. https://doi.org/10.1016/j.msea.2014.03.069
8. Vellingiri S. 2019. An experimental and investigation on the micro-structure hardness and tensile properties of Al-Gr-$Fe_3O_4$ hybrid metal matrix composites. *FME Trans* 47(3): 511-517. https://doi.org/10.5937/fmet1903511S
9. Venkatesh B, Sandeep P, Ramakrishna MVA. 2019. Synthesis and mechanical characterization of magnesium reinforced with SiC composites. *Mater Today Proc* 19: 792-797. https://doi.org/10.1016/j.matpr.2019.08.133
10. Wang T, Wang Y, Bian L, Huang Q. 2019. Microstructural evolution and mechanical behavior of Mg/Al laminated composite sheet by novel corrugated rolling and flat rolling. *Mater Sci Eng A* 765: 138318. https://doi.org/10.1016/j.msea.2019.138318
11. Huang SJ, Abbas A, Ballóková B. 2019. Effect of CNT on microstructure, dry sliding wear and compressive mechanical properties of AZ61 magnesium alloy. *J Mater Res Technol* 8(5): 4273-4286. https://doi.org/10.1016/j.jmrt.2019.07.037
12. Abbas A, Huang SJ, Ballóková B, Sülleiová K. 2020. Tribological effects of carbon nanotubes on magnesium alloy AZ31 and analyzing aging effects on CNTs/AZ31 composites fabricated by stir casting process. *Tribol Int* 142: 105982. https://doi.org/10.1016/j.triboint.2019.105982
13. Vahedi F, Zarei-Hanzaki A, Salandari-Rabori A, Abedi HR, Razaghian A, et al. 2020. Microstructural evolution and mechanical properties of thermomechanically processed AZ31 magnesium alloy reinforced by micro-graphite and nano-graphene particles. *J Alloys Compd* 815: 152231. https://doi.org/10.1016/j.jallcom.2019.152231
14. Jin Y, Wang K, Wang W, Peng P, Zhou S, et al. 2019. Microstructure and mechanical properties of AE42 rare earth-containing magnesium alloy prepared by friction stir processing. *Mater Charact* 150: 52-61. https://doi.org/10.1016/j.matchar.2019.02.008
15. Deng K, Shi J, Wang C, Wang X, Wu Y, et al. 2012. Microstructure and strengthening mechanism of bimodal size particle reinforced magnesium matrix composite. *Compos Part A Appl Sci Manuf* 43(8): 1280-1284. https://doi.org/10.1016/j.compositesa.2012.03.007
16. Zang Q, Chen H, Zhang J, Wang L, Chen S, et al. 2021. Microstructure, mechanical properties and corrosion resistance of AZ31/GNPs composites prepared by friction stir processing. *J Mater Res Technol* 14: 195-201. https://doi.org/10.1016/j.jmrt.2021.06.052
17. Subramani M, Tzeng YC, Tseng LW, Tsai YK, Chen GS, et al. 2021. Hot deformation behavior and processing map of AZ61/SiC composites. *Mater Today Commun* 29: 102861. https://doi.org/10.1016/j.mtcomm.2021.102861
18. Sunil BR, Ganesh KV, Pavan P, Vadapalli G, Swarnalatha C, et al. 2016. Effect of aluminum content on machining characteristics of AZ31 and

AZ91 magnesium alloys during drilling. *J Magnes Alloys* 4(1): 15-21. https://doi.org/10.1016/j.jma.2015.10.003

19. Hu Z, Liu RL, Kairy SK, Li X, Yan H, et al. 2019. Effect of Sm additions on the microstructure and corrosion behavior of magnesium alloy AZ91. *Corros Sci* 149: 144-152. https://doi.org/10.1016/j.corsci.2019.01.024
20. Singh N, Singh J, Singh B, Singh N. 2018. Wear behavior of $B_4C$ reinforced AZ91 matrix composite fabricated by FSP. *Mater Today Proc* 5(9): 19976-19984. https://doi.org/10.1016/j.matpr.2018.06.364
21. Patle H, Sunil BR, Dumpala R. 2020. Sliding wear behavior of AZ91/$B_4C$ surface composites produced by friction stir processing. *Mater Res Express* 7(1): 016586. https://doi.org/10.1088/2053-1591/ab6a55
22. Mohammadi H, Emamy M, Hamnabard Z. 2019. The microstructure, mechanical and wear properties of AZ91-x% $B_4C$ metal matrix composites in as-cast and extruded conditions. *Mater Res Express* 6(12): 126522. https://doi.org/10.1088/2053-1591/ab5405
23. Patle H, Ratna Sunil B, Anand Kumar S, Dumpala R. 2022. Effects of inert gas environment on the sliding wear behavior of AZ91/$B_4C$ surface composites. *Proc Inst Mech Eng Part J J Eng Tribol* 236(9): 1880-1888. https://doi.org/10.1177/13506501211004790
24. Chinthamani S, Kannan G, George GD, Sreedharan CES, Rajagopal KS. 2020. Effect of nano $B_4C$ on the tribological behaviour of magnesium alloy prepared through powder metallurgy. *Mater Sci* 26(4): 392-400. https://doi.org/10.5755/j01.ms.26.3.21556
25. Pitchayyapillai G, Mohamed MJS, Dhanraj G, Prince RMR, Rajeshwaran M, et al. 2022. Influence of $B_4C$ on mechanical properties of AZ91 magnesium matrix composites. *Mater Today Proc* 59: 1438-1441. https://doi.org/10.1016/j.matpr.2021.12.135
26. Jeffrey JA, Kumar SS, Roseline VA, Mary AL, Santhosh D. 2022. Contriving and assessment of magnesium alloy composites augmented with boron carbide VIA liquid metallurgy route. *Mater Sci Forum* 1048: 3-8. https://doi.org/10.4028/www.scientific.net/MSF.1048.3
27. Khatkar SK, Verma R, Sumankant, Kharb SS, Thakur A, et al. 2021. Optimization and effect of reinforcements on the sliding wear behavior of self-lubricating AZ91D-SiC-Gr hybrid composites. *Silicon* 13: 1461-1473. https://doi.org/10.1007/s12633-020-00523-0
28. Sahoo BN, Khan F, Babu S, Panigrahi SK, Ram GJ. 2018. Microstructural modification and its effect on strengthening mechanism and yield asymmetry of *in-situ* TiC-$TiB_2$/AZ91 magnesium matrix composite. *Mater Sci Eng A* 724: 269-282. https://doi.org/10.1016/j.msea.2018.03.060
29. Aydin F, Sun Y, Emre Turan M. 2019. The effect of $TiB_2$ content on wear and mechanical behavior of AZ91 magnesium matrix composites produced by powder metallurgy. *Powder Metall Met Ceram* 57: 564-572. https://doi.org/10.1007/s11106-019-00016-9
30. Deng KK, Wu K, Wu YW, Nie KB, Zheng MY. 2010. Effect of submicron size SiC particulates on microstructure and mechanical properties of AZ91 magnesium matrix composites. *J Alloys Compd* 504(2): 542-547. https://doi.org/10.1016/j.jallcom.2010.05.159
31. Zhang L, Wang Q, Liu G, Guo W, Jiang H, et al. 2017. Effect of SiC particles and the particulate size on the hot deformation and processing map of AZ91 magnesium matrix composites. *Mater Sci Eng A* 707: 315-324. https://doi.org/10.1016/j.msea.2017.09.056
32. Guler O, Say Y, Dikici B. 2020. The effect of graphene nano-sheet (GNS) weight percentage on mechanical and corrosion properties of AZ61 and AZ91 based magnesium matrix composites. *J Compos Mater* 54(28): 4473-4485. https://doi.org/10.1177/0021998320933345
33. Arivukkarasan S, Dhanalakshmi V, Stalin B, Ravichandran M. 2018. Mechanical and tribological behaviour of tungsten carbide reinforced aluminum LM4 matrix composites. *Part Sci Technol* 36(8): 967-973. https://doi.org/10.1080/02726351.2017.1331285
34. Suresh V, Praneet AD, Anoop J. 2021. Ingenious analysis on machining parameters of aluminium alloy (LM25)/graphite (Gr)/boron carbide ($B_4C$) hybrid composites using wire electrical discharge machining (WEDM). *Mater Today Proc* 37: 3112-3117. https://doi.org/10.1016/j.matpr.2020.09.021
35. Mishra AK, Sheokand R, Srivastava RK. 2012. Tribological behaviour of Al-6061/SiC metal matrix composite by Taguchi's techniques. *Int J Sci Res Publ* 2(10): 1-8.
36. Suresh V, Vikram P, Palanivel R, Laubscher RF. 2018. Mechanical and wear behavior of LM25 aluminium matrix hybrid composite reinforced with boron carbide, graphite and iron oxide. *Mater Today Proc* 5(14): 27852-27860. https://doi.org/10.1016/j.matpr.2018.10.023
37. Ranjith R, Giridharan PK. 2015. Experimental investigation of surface hardness and dry sliding wear behavior of AA7050/$B_4C_p$. *High Temp Mater Process* 19(3-4): 291-305. https://doi.org/10.1615/HighTempMatProc.2016016824
38. Sardar S, Karmakar SK, Das D. 2018. Evaluation of abrasive wear resistance of $Al_2O_3$/7075 composite by Taguchi experimental design technique. *Trans Indian Inst Met* 71: 1847-1858. https://doi.org/10.1007/s12666-018-1317-9
39. Chelladurai SJS, Arthanari R, Nithyanandam N, Rajendran K, Radhakrishnan KK. 2018. Investigation of mechanical properties and dry sliding wear behaviour of squeeze cast LM6 aluminium alloy reinforced with copper coated short steel fibers. *Trans Indian Inst Met* 71: 813-822. https://doi.org/10.1007/s12666-017-1258-8
40. Senthil Kumar BR, Gopalarama Subramaniyan G, Pragadish N, Venkatesh PM, Sanjay S, et al. 2022. Investigations on wear behavior of aluminium composites at elevated temperature. *Adv Mater Sci Eng* 2022: 9594798. https://doi.org/10.1155/2022/9594798
41. Lu YQ, Zhu XJ, Hu XD, Yao Y, Cai H. 2017. Effects of blowing Ar on inclusion and properties of AZ61 magnesium alloy. *Key Eng Mater* 725: 416-420. https://doi.org/10.4028/www.scientific.net/KEM.725.416
42. Avvari M, Narendranath S, Able M. 2016. Microstructure evolution in AZ61 alloy processed by equal channel angular pressing. *Adv Mech Eng* 8(6): 1-6. https://doi.org/10.1177/1687814016651820
43. Alavi Nia A, Nourbakhsh SH. 2016. Microstructure and mechanical properties of AZ31/SiC and AZ31/CNT composites produced by friction stir processing. *Trans Indian Inst Met* 69(7): 1435-1442. https://doi.org/10.1007/s12666-015-0702-x
44. Aatthisugan I, Rose AR, Jebadurai DS. 2017. Mechanical and wear behaviour of AZ91D magnesium matrix hybrid composite reinforced with boron carbide and graphite. *J Magnes Alloys* 5(1): 20-25. https://doi.org/10.1016/j.jma.2016.12.004